Title

Metformin intervention prevents cardiac dysfunction in a murine model of adult congenital heart disease.

Authors

Wilmanns, Julia C
Pandey, Raghav
Hon, Olivia
et al.

Publication Date

2019-02-01

DOI

10.1016/j.molmet.2018.11.002

Peer reviewed

Original Article

MOLECULAR METABOLISM

Metformin intervention prevents cardiac dysfunction in a murine model of adult congenital heart disease

Julia C. Wilmanns [2,3,13], Raghav Pandey [1,13], Olivia Hon [1], Anjana Chandran [2], Jan M. Schilling [4], Elvira Forte [1], Qizhu Wu [5], Gael Cagnone [6], Preeti Bais [1], Vivek Philip [1], David Coleman [1], Heidi Kocalis [1], Stuart K. Archer [7,8], James T. Pearson [5,9,10], Mirana Ramialison [2,11], Joerg Heineke [3], Hemal H. Patel [4], Nadia A. Rosenthal [1,2,12], Milena B. Furtado [1,2], Mauro W. Costa [1,2,*]

ABSTRACT

Objective: Congenital heart disease (CHD) is the most frequent birth defect worldwide. The number of adult patients with CHD, now referred to as ACHD, is increasing with improved surgical and treatment interventions. However the mechanisms whereby ACHD predisposes patients to heart dysfunction are still unclear. ACHD is strongly associated with metabolic syndrome, but how ACHD interacts with poor modern lifestyle choices and other comorbidities, such as hypertension, obesity, and diabetes, is mostly unknown.

Methods: We used a newly characterized mouse genetic model of ACHD to investigate the consequences and the mechanisms associated with combined obesity and ACHD predisposition. Metformin intervention was used to further evaluate potential therapeutic amelioration of cardiac dysfunction in this model.

Results: ACHD mice placed under metabolic stress (high fat diet) displayed decreased left ventricular ejection fraction. Comprehensive physiological, biochemical, and molecular analysis showed that ACHD hearts exhibited early changes in energy metabolism with increased glucose dependence as main cardiac energy source. These changes preceded cardiac dysfunction mediated by exposure to high fat diet and were associated with increased disease severity. Restoration of metabolic balance by metformin administration prevented the development of heart dysfunction in ACHD predisposed mice.

Conclusions: This study reveals that early metabolic impairment reinforces heart dysfunction in ACHD predisposed individuals and diet or pharmacological interventions can be used to modulate heart function and attenuate heart failure. Our study suggests that interactions between genetic and metabolic disturbances ultimately lead to the clinical presentation of heart failure in patients with ACHD. Early manipulation of energy metabolism may be an important avenue for intervention in ACHD patients to prevent or delay onset of heart failure and secondary comorbidities. These interactions raise the prospect for a translational reassessment of ACHD presentation in the clinic.

Keywords Adult congenital heart disease; Metabolism; Obesity; Metformin

1. INTRODUCTION

Successful corrective interventions for CHD malformations have led to improved patient survival into adulthood, causing a staggering 60% increase in patients presenting with adult congenital heart disease (ACHD) [1,2]. Consequently, the number of ACHD genetically predisposed individuals is on the rise, affecting approximately 2.4 million patients in the US alone [2]. Although early corrective interventions for CHD are successful, CHD patients have a higher risk of developing progressive cardiac dysfunction during adulthood. Among the ACHD population the prevalence of comorbidities such as renal, pulmonary, hepatic, and vascular dysfunctions, as well as psychiatric diagnosis are elevated. These major health risks drastically increase the morbidity and mortality of ACHD patients [3]. The high prevalence of associated metabolic disorders in ACHC also merits further investigation, given the multiple prophylactic options currently available in the clinic.

[1]The Jackson Laboratory, USA [2]Australian Regenerative Medicine Institute, Monash University, Australia [3]Department of Cardiology and Angiology, Experimental Cardiology, Hannover Medical School, Germany [4]VA San Diego Healthcare System and Department of Anesthesiology, University of California San Diego, USA [5]Monash Biomedical Imaging, Monash University, Australia [6]Department of Pharmacology, Research Center of CHU Sainte-Justine, Canada [7]Monash Bioinformatics Platform, Monash University, Australia [8]Biomedicine Discovery Institute, Faculty of Medicine, Nursing and Health Sciences, Monash University, Australia [9]Department of Physiology, Monash University, Australia [10]National Cerebral & Cardiovascular Center, Suita 565-8565, Japan [11]Systems Biology Institute, Australia [12]National Heart and Lung Institute, Imperial College London, W12 0NN, UK

[13] These authors contributed equally to the work.

*Corresponding author. The Jackson Laboratory, 600 Main St, Bar Harbor, ME 04609, USA. Fax: +1 207 288 6281. E-mail: mauro.costa@jax.org (M.W. Costa).

Received August 21, 2018 • Revision received November 6, 2018 • Accepted November 10, 2018 • Available online 15 November 2018

https://doi.org/10.1016/j.molmet.2018.11.002

The continuous decline in physical activity and increased caloric intake has resulted in an obesity epidemic in developed countries that is the major health risk of the 21st century. It is estimated that approximately 63.3% of the American population is currently overweight or obese [4]. ACHD intrinsic congenital heart dysfunction is exacerbated by external environmental factors, including obesity, diabetes, and/or high blood pressure, all of which can trigger heart failure [5–7]. Therefore, it is imperative to understand why today's lifestyle set ACHD patients at an even higher, life-threatening risk than the general population. Despite the existence of large epidemiological datasets, not much is currently known about how ACHD predisposes patients to heart failure upon metabolic stress. The present study focuses on how obesity affects cardiac function in our recently characterized ACHD model [8,9]. Using genetically predisposed mice [9] and diet as a cardiac stressor, we describe a preexistent imbalance in the metabolic state of ACHD hearts. Development of obesity increases the severity of heart dysfunction. This interaction between genetic and metabolic factors ultimately leads to the clinical presentation of heart failure in ACHD. Modulation of energy utilization by Metformin, a drug widely used to treat type 2-diabetes, prevents cardiac dysfunction in ACHD/obesity model and could therefore be considered a preventive intervention for heart failure in ACHD. Our observations also suggest that ACHD is a complex, multifactorial disease that can be modulated by changes in global metabolism. Patients at risk for ACHD show intrinsic metabolic dysfunction that is aggravated by exposure to a modern lifestyle environment leading to cardiac dysfunction, and therefore should be differentially monitored.

2. METHODS

2.1. Mouse lines

Nkx2-5$^{C/+}$ and Nkx2-5$^{183P/+}$ (ACHD) heterozygous mice have been previously characterized [9]. All mice were maintained on a C57BL/6J background, housed at Monash Animal Services, Australia, or at The Jackson Laboratory, USA. This investigation conforms with the Guide for the Care and Use of Laboratory Animals published by the US National Institutes of Health (NIH Publication No. 85–23, revised 1996) and requirements under the ethics application MARP-2011-175 (Monash University) and ACUC 16011 (The Jackson Laboratory). Control mice used were either *Nkx2-5$^{C/+}$* (homologous recombination replacing the I residue with itself; i.e. control = C) or wild-type (WT). No significant molecular or physiological differences were observed between these two control groups [9]. Whenever possible, control littermates were used for the experiments. All experiments were performed on adult males.

2.2. Feeding regimen

Six-week-old male mice were subdivided into four experimental groups according to genotype and feeding regimen (control Low Fat (LF), control High Fat (HF); ACHD LF and ACHD HF). Throughout the study, two time-point cohorts were used: short (weeks 6–15) and long (weeks 6–30) feeding regimens. All mice were single housed under normal environmental conditions (21.5 ± 1 °C with a light–dark cycle of 12 h:12 h). For metformin studies, four siblings male mice were housed together during treatment. Food and water were accessible *ad libitum*. Low Fat diet (SF13-081/D12451; total calculated digestible energy from lipids: 12.0%, total calculated digestible energy from protein: 25.8%) and High Fat diet (SF04-001; total calculated digestible energy from lipids: 43.0%, total calculated digestible energy from protein: 21.0%) were purchased from Specialty Feeds, Pty Ltd. (Australia) and Research Diets Inc. (USA). Metformin at the concentration of 5 mg/mL was added to the water from 8 weeks of age until the end of the protocol *at libitum*. Weight and food consumption were recorded weekly at 10 a.m ± 2 h from the age of 6 weeks until week 15 for short feeding regimen groups and further calculated at week 30 for long feeding regimen groups.

2.3. Histology

Mice were euthanized via CO_2 asphyxiation, perfused with HBSS (Thermo), followed by heart dissection. Hearts were further incubated for 5 min in 60 mM KCl for synchronization of heart cycle before fixation. Tissues were fixed in 4% PFA at 4 °C overnight and further processed for paraffin sectioning following standard dehydration and embedding protocols. Adult thyroids were sectioned at 14 μm thickness, adult hearts at 10 μm thickness. Masson's Trichrome staining was performed by the Monash Histology Facility. For myocyte area measurements, transverse sections were stained with Wheat Germ Agglutinin Alexafluor 488 conjugate (WGA, Thermo). All images were obtained using Olympus DotSlide (Japan). Mitochondrial density was analyzed by immunofluorescence on 20 μm heart cryosections using TOMM20 rabbit polyclonal antibody (Abcam) raised against the *Translocase of Outer Protein Membrane 20* gene (*Tomm20*). Confocal Z-stack images were performed using Leica SP8. Myocyte area and fluorescent intensity were measured using FIJI software with three replicates for each genotype. For TEM, 50 mg of cardiac tissue was processed by the JAX histology core, and sections were evaluated using JM-1230 microscope (JEOL) coupled to AMT 2K camera (Advanced Microscopy Techniques). Statistical significance of data was determined by ANOVA or Student's t-test.

2.4. Magnetic Resonance Imaging (MRI), Echocardiography and ECG analysis of cardiac function

15- and 30-week old adult mice were anesthetized with 2% ± 0.2% isoflurane for non-invasive imaging in a prone position. For MRI, imaging was performed in spontaneously breathing mice in a 9.4 T MRI scanner (Agilent, USA) to assess left ventricular and right ventricular chamber dimensions in systole and diastole using T1 and T2-weighted anatomical sequences. Breathing was also monitored to avoid measurement distortions during the breathing cycle. Measurements of cardiac function were performed using Segment software [10] analyzed blinded to genotype by two independent researchers. Echocardiogram analysis was performed using Vevo 2100 (FUJIFILMS Visualsonics). ECG was recorded in anesthetized mice using Powerlab data acquisitions system (ADInstruments, USA) and analyzed using LabChart8 software (ADInstruments, USA).

2.5. Metabolic measurements

For accurate measurement of weight and body fat composition, we performed dual-energy X-ray absorptiometry (DeXa) using Lunar PIXImus Densitometer (GE Medical Systems, USA) or Echo MRI™ (USA). For DeXa analysis, mice were anesthetized with 1.7% ± 0.2% isoflurane. Whole-body metabolic changes in activity and energy expenditure were assessed using individually housed animals in the comprehensive cage monitoring system Promethion (Sable Systems International, USA). Mice were maintained on a 12 h light:dark cycle with access to food and water *ad libitum* in cages undisturbed for 120 h to collect CO_2 production, O_2 consumption, locomotor activity, body mass, and food and water intake. Voluntary exercise capacity in running wheels (Med Associates Inc, USA) was measured by recording running distance and circadian activity for 5 continuous days. Metabolite levels of cholesterol, triglycerides, glucose and NEFA were

quantified from mouse sera using the Clinical Assessment Services, The Jackson Laboratory.

2.6. Adult cellular respiration analysis

Mitochondrial function in mechanically permeabilized fibers from the left ventricular free wall was evaluated using the Oxygraph-2k Respirometer (Oroboros Instruments, AT). Fibers were added to the oxymetry chamber containing MiR06 media (EGTA 0.5 mM, $MgCl_2$ $6H_2O$ 3 mM, Lactobionic acid 60 mM, Taurine 20 mM, KH_2PO_4 10 mM, HEPES 20 mM, D-Sucrose 110 mM, BSA 1 g/l, Catalase 280 U/ml, pH 7.1, at 30 °C) with 25 μM Blebbistatin [11]. Fatty acid oxidation and Complex I protocols were adapted from a previously published protocol [12] and depicted in Figure 4E.

2.7. Metabolomics and western blot analysis

Unbiased discovery metabolite platform was performed at the West Coast Metabolomics Center (UC Davis, USA). Biventricular apex fragments were snap frozen in N_2 and shipped to the Center in dry ice. The metabolomics platform used consisted of four different combinations of liquid chromatography (LC) and mass spectrometry ionization using Agilent 6890 GC (Agilent Technologies, USA) followed by Pegasus III TOF MS (LECO corporation, USA). Relative abundance of 273 unique metabolic features (109 metabolites of known structures and 164 unique features of unknown structure), normalized to internal standards were measured at each time point. Metaboanalyst 3.0 software [13] was used for bioinformatics analysis. Interquartile range based filtering was used to remove features unlikely to be used for modeling purposes [14]. The data were log transformed and autoscaled [15]. Fold Change (FC) analysis (before column normalization), t-tests, and volcano plots were generated comparing the mutant samples with the control samples at each time point. Protein changes were analyzed by western blot using proteins extracted from biventricular fragments as previously described [9]. Antibodies used are described in Supplementary Table 4.

2.8. Functional annotation enrichment analysis of Nkx2-5 ChIP peak regions

Publicly available chromatin immunoprecipitation followed by deep-sequencing (ChIP-seq) data (GSE35151) [16] was re-analyzed by our group. Unsupervised enrichment analysis of genome-wide occupancy profile of Nkx2-5 in adult mouse whole heart was performed using Genomic Regions Enrichment of Annotations Tool [17]. We performed gene ontology (GO) analysis using GREAT default setting (5 kb proximal + 1 kb basal, up to 1 Mb distal, mm9 reference genome) calculating statistical enrichments by associating genomic regions with nearby genes and applying the gene annotations to the regions.

2.9. RNAseq, bioinformatics and validation

Ventricular heart samples from 15-week old adult males of each genotype (*Nkx2-5*$^{183C/+}$, WT, and *Nkx2-5*$^{183P/+}$ mice) on a high fat diet were used as biological replicates for RNA sequencing. Total RNA extraction was performed using the mirVana kit (Thermo, USA) and cleared of genomic DNA contamination using in column DNAse treatment (Qiagen, Germany). Samples were further processed by the Medical Genomics Facility at Monash University. RNA-seq data (paired-end reads of 100 nt) were trimmed for quality and adapter contamination using Cutadapt [18] as implemented in Trim Galore (Phred quality threshold of 28, minimum adapter overlap 3 nt, adaptor sequence AGATCGGAAGAGC). It was then mapped to the mouse genome (mm10) using STARv2.4.0 [19], and reads were tallied within gene features using HTSeq [20]. From the resulting read-count matrix, genes with more than 10 reads in any sample were kept and differentially expressed genes were called using limma.voom [21]. Targets with a FDR cut-off of 0.1 were further selected for validation using qPCR. cDNA synthesis was performed in the same samples using Superscript VILO (Thermo) followed by SYBR green reactions (Roche, USA) and analyzed using the LightCycler480 (Roche, USA). Relative quantification was obtained using *Hprt* as a normalizer. Primers used are described in Supplementary Table 4. Ingenuity Pathway Analysis (IPA) software (Qiagen Bioinformatics, Germany) was used to analyze differentially regulated pathways and functions in datasets.

2.10. Statistics

Data as presented as a mean ± SEM. Statistical significance of data was determined by ANOVA and Student's t-test. P values < 0.05 were considered significant.

3. RESULTS

3.1. ACHD mice show increased susceptibility to weight gain and development of obesity

In a previous study, we described a point mutation in the *NKX2-5* gene found in a familial ACHD cohort. We engineered the same human mutation in mice and showed that our model reproduced all clinical features of the disease [9]. To explore the interplay between ACHD, metabolism, and heart function, we subjected ACHD mice to control conditions under low fat (LF) and high fat (HF) diet as a metabolic stressor (Figure 1A). At the onset of the feeding regimen (6 weeks of age), ACHD mice had significantly lower weight when compared to control mice (Supplementary Figure 1). Surprisingly, after 9 weeks of diet, ACHD mice showed a significantly higher weight gain when compared to control mice on HF diet. The increased weight gain was attributed to higher body fat, as lean body weight did not differ between groups (Figure 1B). No difference in weight was observed between experimental groups subjected to LF diet. In summary, ACHD mice showed comparatively higher fat accumulation and weight gain when subjected to higher caloric intake, indicating that ACHD and diet have combined additive effects on weight gain and therefore ACHD mice are more predisposed to develop obesity.

3.2. Obesity triggers cardiac dysfunction in ACHD

We have previously shown that most disease features developed in the ACHD model are functionally compensated in homeostasis in early adulthood [9], except for RV dysfunction, defined by a significant decrease of right ventricular ejection fraction (EF) (Figure 1C,D). Short-term 9-week HF feeding regimen (15 weeks of age) did not significantly affect cardiac function (Figure 1D, Supplementary Figure 2A). However, the long-term 24-week regimen (30 weeks of age) caused a significant decrease in EF for both right (RV) and left (LV) ventricles, as well as enhanced RV and right atrial (RA) dilation in ACHD mice (Figure 1C,D; Supplementary Figure 2B). Once subjected to HF diet, murine ACHD hearts showed increased wall thickness, eccentric ventricular hypertrophy with dilation, and an increase in transverse myocyte area (Figure 1E,F). Hypertrophy was also evident in ACHD mice subjected to LF diet but was enhanced on HF diet. No hypertrophy was seen in control mice independent of the diet of choice, demonstrating the importance of genetic predisposition for the hypertrophic response. In summary, ACHD mice showed several morphological abnormalities and cardiac dysfunction prior to the development of Heart Failure with Preserved Ejection Fraction (HFpEF) [22] when subjected to metabolic stress (HF diet), suggesting that challenging a weakened ACHD heart with metabolic stress accelerates progression to heart failure.

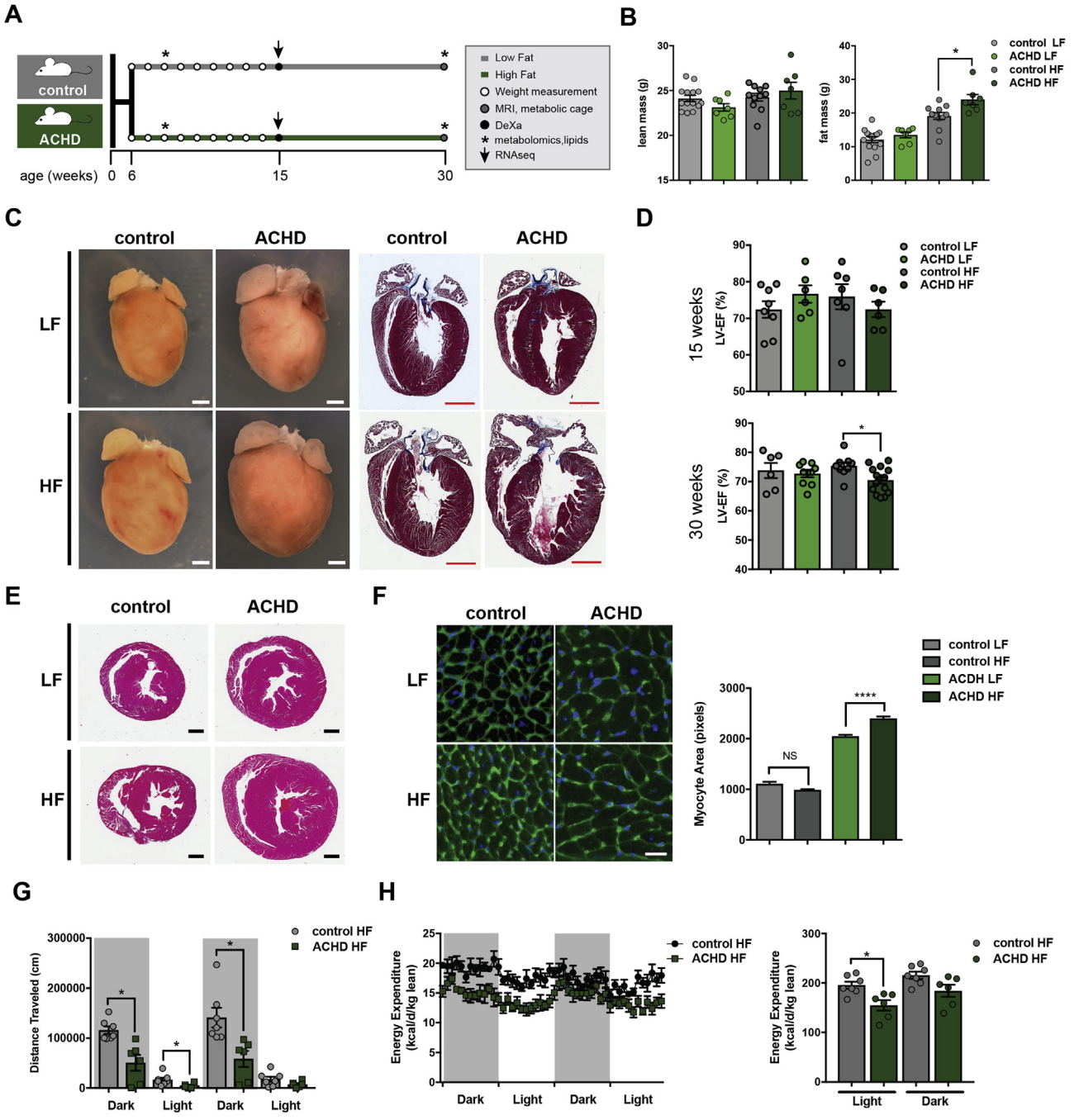

Figure 1: Effect of high fat diet on ACHD hearts and body metabolism. (A) Experimental design, treatment groups, and analyses end-points. (B) Lean and fat mass measurements of body weight for control and ACHD mice under low (LF) and high (HF) diet at the 30-week time-point. (C) Whole-mount view and trichrome stained histological sections of control and ACHD hearts at 30 weeks. (D) Left-ventricular (LV) ejection fraction (EF) measurements of cardiac function of control and ACHD animals under LF and HF diets at the early (15-week) and late (30-week) time-points. (E–F) Transverse hematoxylin and eosin stained sections (E) and quantification of myocyte cross-sectional area of WGA and DAPI stained sections (F) of control and ACHD animals under LF and HF diets at the 30-week time-point. (G–H) Running capacity and energy expenditure of ACHD and control mice under LF and HF at 30 weeks, showing distance traveled (G) and energy expenditure (H) during dark (active) and light (resting) light cycles. N = 6 per experimental group; Mean ± SEM, Student's t-test; *p < 0.05; **p < 0.01; ****p < 0.0001.

3.3. Obesity triggers global metabolic energy dysfunction in ACHD mice

When provided with voluntary running exercise, ACHD mice on HF diet at 30 weeks displayed significantly reduced physical performance, as measured by decreased running distance (dark cycle; Figure 1G). No significant changes were detected in time spent on the wheel, food intake and activity, indicating that ACHD mice were active but not running at the same speed as control mice (Supplementary Figure 3A,B). Overall energy expenditure of mice on HF diet was also significantly reduced in ACHD mice (Figure 1H), with decreased levels of O_2 consumption (volume O_2 – VO_2) and CO_2 production (volume CO_2 – VCO_2) rates, while still maintaining normal respiratory

exchange ratio (RER). These changes were not observed when ACHD mice were subjected to a Western diet formulation (manuscript under preparation), which contains high sugar [23], indicating that cardiac dysfunction was likely mediated by increased availability of fatty acids in the HF diet. Together, these data confirm that nutritional imbalance exacerbates heart dysfunction in ACHD mice.

To determine how global metabolism was affected, we monitored serum levels of glucose and lipids of ACHD mice on HF diet. While no significant changes were seen at 6 weeks, higher plasma levels of triglycerides and a tendency towards increased cholesterol and free fatty acids (NEFA) at 30 weeks was observed (Figure 2A). Glucose handling was also affected in ACHD mice on HF diet, with an improved response when compared to control mice (Figure 2B, Supplementary Figure 4).

3.4. Primary heart metabolic dysfunction in ACHD mice is driven by changes in energetic substrates

NKX2-5 is a transcription factor essential for heart formation during embryonic development, although the molecular consequences of its dysfunction in adult hearts are still largely unknown. Analysis of chromatin immunoprecipitation followed by deep-sequencing (ChIP-seq) of adult hearts using gene ontology (GO) and molecular signature database (MSigDB) revealed that the human NKX2-5 protein binds the promoter regions of essential genes associated with cellular metabolism and energy production (Figure 3A, Supplementary Table 1), a previously unrecognized phenomenon. To further explore the molecular mechanisms underlying the primary metabolic alterations in ACHD hearts, we performed transcriptome analysis (RNAseq) on short-term HF-fed mice, before cardiac dysfunction was established. This analysis focused on investigation of genes that were differentially expressed between obese control and ACHD mice, to expose molecular differences of the metabolic stress model (ACHD + obesity). Relative quantification showed 1264 genes differentially expressed between control and ACHD obese hearts. Ingenuity Pathway Analysis (Qiagen) revealed 41 predicted upstream regulators of affected genes (Figure 3B), including cardiac transcription factors known to partner with NKX2-5, four of which are involved in cardiogenesis and cardiac function. The canonical pathway of cardiac hypertrophy was significantly changed in ACHD (z-score = −1.347; p-value = 0.00011), confirming our finding of eccentric hypertrophy (Figure 1E,F).

Among genes involved in the hypertrophic response, *Rock* and *Mlc* complexes and a large subset of other effector genes such as *Gata4*,

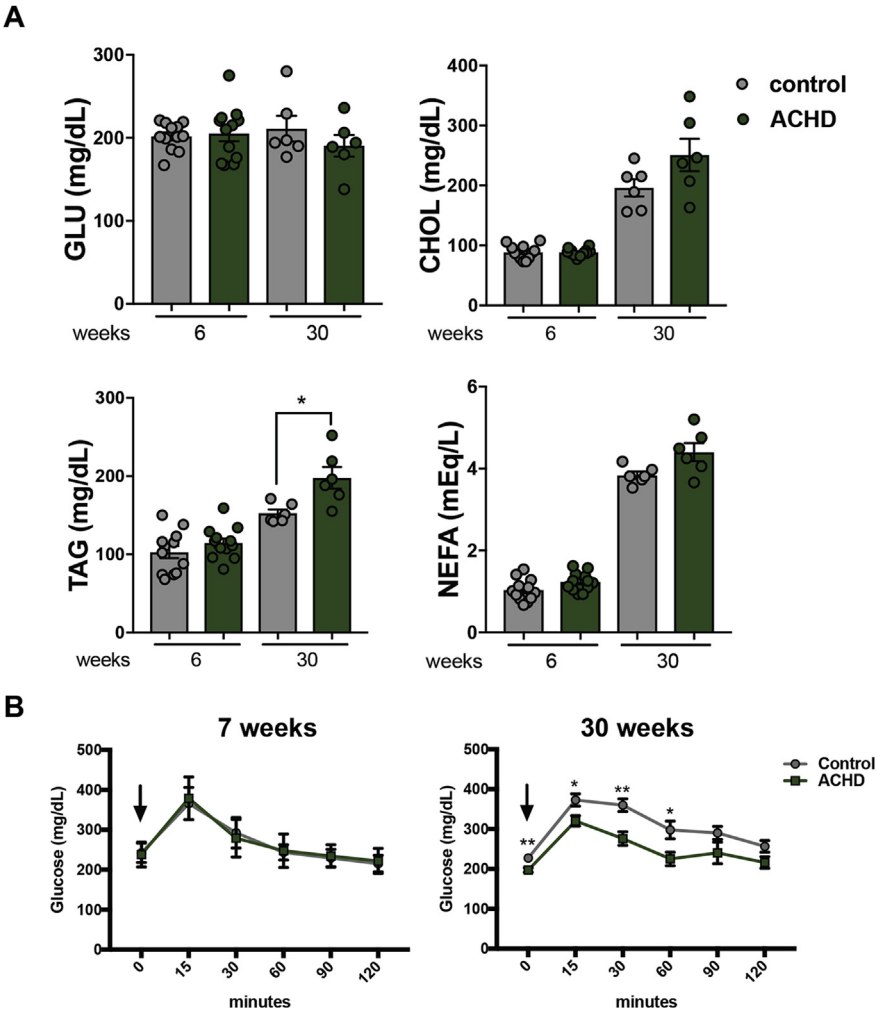

Figure 2: Metabolic disturbances in ACHD hearts under high fat diet. (A) Serum glucose, lipid analyses, and (B) glucose tolerance test (GTT) in ACHD and control mice at 6 weeks (before start of diet) 30 weeks (long-term diet end-point). N ≥ 6, Mean ± SEM, Student's t-test, *p < 0.05, **p < 0.01. GLU — glucose; CHOL — cholesterol; TAG — triglycerides; NEFA — non-esterified free fatty acid.

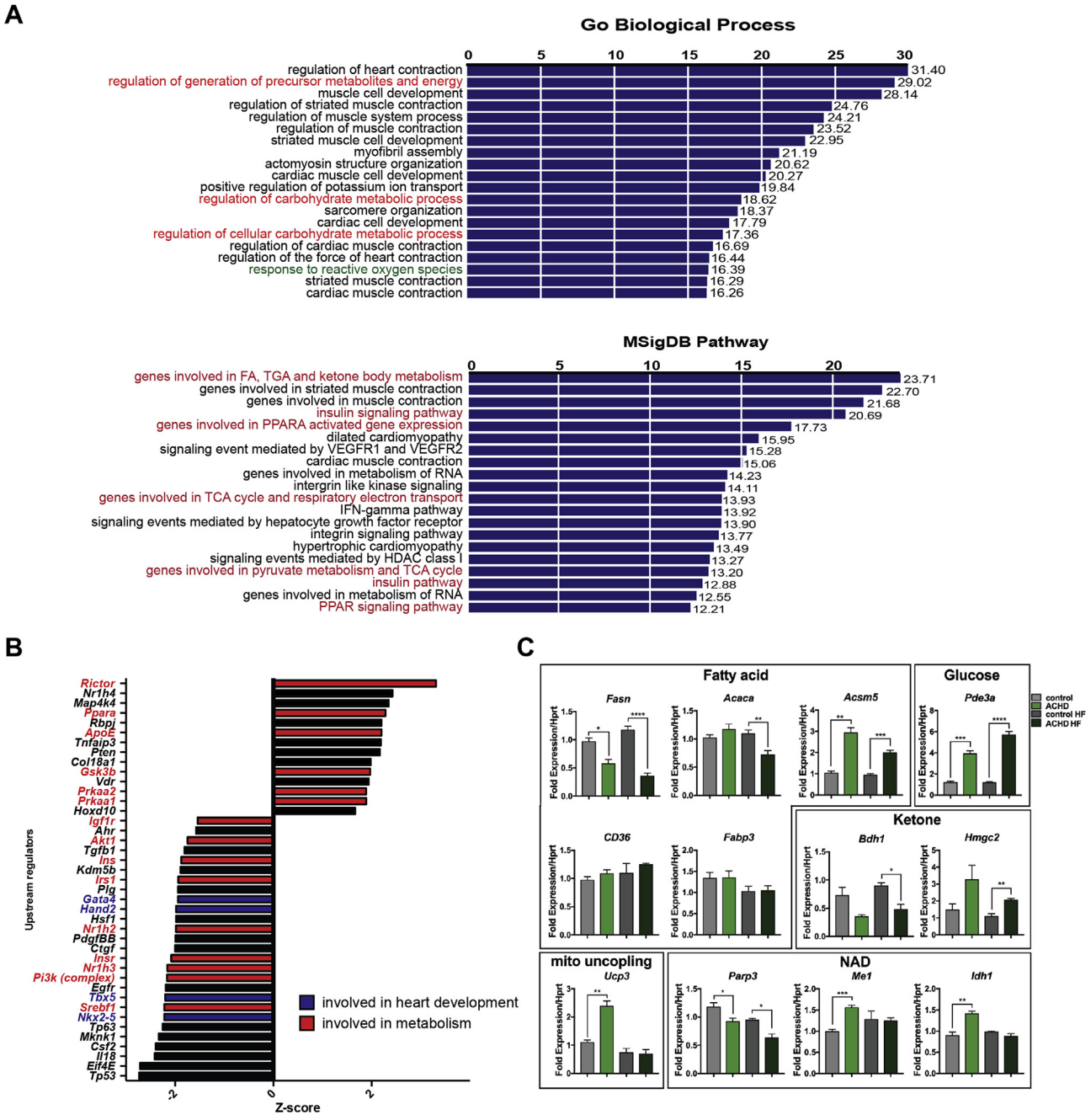

Figure 3: NKX2-5 regulates energy handling in adult hearts. (A) Bioinformatics analyses of ChIP-seq against NKX2-5 in adult hearts (GEO GSE5151). Genes involved in metabolism are highlighted in red in both Go Biological Process and Molecular Signature Database (MSigDB) resources. (B). Ingenuity Pathway Analysis (IPA) of genes differentially regulated in obese ACHD heart RNAseq data reveals various upstream regulators for metabolism (red) and heart development (blue) processes. (C) qPCR validation of RNAseq data, showing differential expression of genes associated with energy flexibility in ACHD mice under LF or HF diet at 15 weeks. Transcripts involved in fatty acid oxidation (*Fasn, Acaca, Acam5, CD36, Fabp3*), glucose handling (*Pde3a*), ketone metabolism (*Bdh1, Hmgc2*), NAD production (*Parp3, Me1, Idh1*) and mitochondrial uncoupling (*Ucp3*) were tested. Data presented as fold expression compared to control samples normalized by *Hprt* levels. N = 3; Mean ± SEM, Student's t-test, *p < 0.05, **p < 0.01; ***p < 0.001, ****p < 0.0001.

Hand2, *Mef2*, and *p300* were up regulated in ACHD mutants (Supplementary Figure 5). These genes trigger an increase in contractility, leading to long-term cardiac hypertrophy [24–28]. Furthermore, *eIF4E* (mRNA cap-binding protein) and *Mlnk1* (eIF4E kinase), known essential regulators of cell size control and global protein synthesis, were also affected in ACHD hearts. Interestingly, 37% of upstream regulators were associated with metabolic pathways and lipid processing, including *Srebf1*, *Nr1h2-3*, *Insr*, and *ApoE*, among others. This analysis corroborates the global whole-body metabolic data, indicating that disturbances in heart metabolism precede progression to heart dysfunction in ACHD.

Another affected pathway was PPAR signaling, where *Ppara*, *Prkaa1*, and *Prkaa2* were highlighted as potential regulators in ACHD mice. These proteins are key components in fatty acid metabolism and are normally activated to compensate for energy deprivation, which is a common feature of heart failure [29,30] (Figure 3B). Transcriptional

changes directly linked to metabolism were further confirmed by qPCR (Figure 3C). In particular, decreased levels of *Fasn* and *Acaca* and increased levels of *Acsm5* indicated marked reduction of fatty acid synthesis and increased fatty acid oxidation, presumably via loss of inhibition of CPT1 [31], whereas *Fabp3* and *CD36* fatty acid receptor transcripts were not changed, suggesting no alteration in fatty acid uptake. In agreement with these observations, increased levels of *Pde3b* suggested enhanced glucose metabolism, although no significant changes were seen in *Insr* expression. Ketone body metabolism gene *Bdh1* showed decreased levels, while *Hmgcs2* was increased [32].

Genes associated with mitochondrial uncoupling/protection (*Ucp3*) and NAD+ metabolism (*Me1*, *Idh1*, and *Parp3*) were also affected. Most of these genes are normally activated in heart failure [30]. These changes in gene expression are likely associated with the shift in energy signature [33,34], indicating that ACHD mice show imbalanced energy utilization, and confirm that metabolic changes in ACHD mice are enhanced by HF diet and precede heart failure.

3.5. Imbalanced cardiomyocyte energy handling capacity precedes heart dysfunction in ACHD

To further characterize molecular mechanisms associated with onset of ACHD progression to heart failure, we performed comprehensive metabolic and physiological analysis in early adulthood, before ACHD mice develop cardiac dysfunction. This allowed us to filter out changes that are not directly caused by cardiac dysfunction. At 8 weeks of age, ACHD mice showed a small but significant decrease in body weight compared to control wild-type mice, associated with decreased lean mass (Supplementary Figure 1), although no changes were observed in energy expenditure, VCO_2/VO_2 consumption or voluntary exercise capacity (Supplementary Figure 6A–C). No significant changes were observed in cardiac electrical activity (Supplementary Figure 7), other than increased spread of the QRS interval, consistent with the well-established role for NKX2-5 in the maintenance of the conduction system in mouse models and patients [35–38]. Echocardiographic (Echo) analysis of heart function showed small changes in left ventricular function but normal ejection fraction, indicating that imbalance of NKX2-5 protein activity can be compensated for to ensure adequate heart function in early adulthood (Supplementary Table 2).

We have previously observed decreased mitochondrial respiratory capacity in neonatal ACHD cardiomyocytes [9]. Therefore, we investigated cellular respiration and energy handling in young ACHD hearts at 8–10 weeks of age. Mitochondrial morphology was not changed in ACHD cardiomyocytes compared with controls (Figure 4A), but a significant decrease in mitochondrial density was observed (Figure 4B–D). In agreement with the data obtained in neonatal cardiomyocytes [9], mitochondrial function in left ventricular free wall fibers of the young adult heart revealed tendency to reduced oxygen flux and fatty acid oxidative capacity in ACHD hearts (Figure 4E). Unbiased global metabolomics (untargeted GCMS analysis) showed a significant

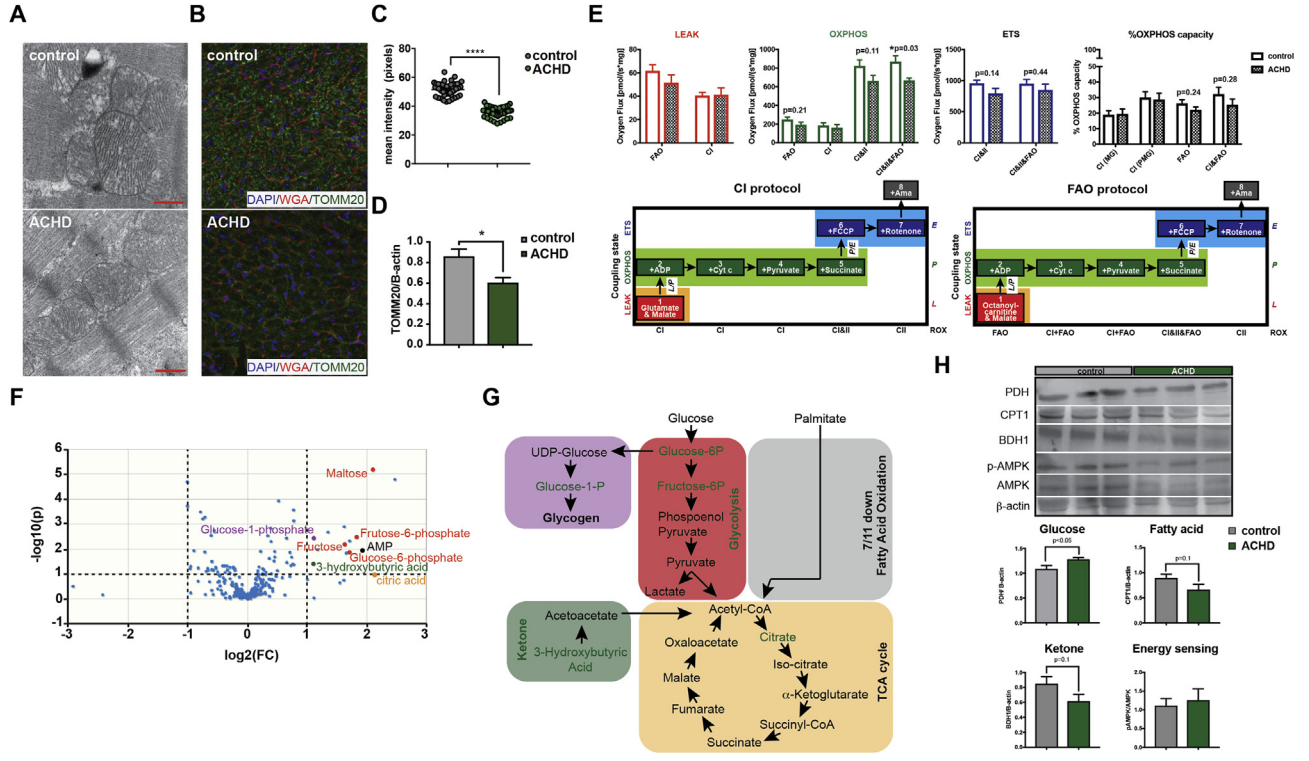

Figure 4: Mitochondrial function and energy handling in ACHD hearts. (A) Transmission electron micrograph of control and ACHD muscle fibers showing size and shape of mitochondria. (B) Confocal imaging of transverse myocardial sections of control and ACHD hearts showing mitochondrial density (green signal – TOMM20) over nuclear staining (DAPI) and cardiomyocyte area staining (red – WGA). (C) Quantification of TOMM20 immunofluorescence or (D) protein expression ACHD and control hearts at 10 weeks (N = 3). (E) OROBOROS O2k Respirometer oxygen flux analysis of ACHD and control hearts. CI = complex I; CII = complex II; FAO = fatty acid oxidation; M = malate, G = glutamate; P = pyruvate; ROX = residual oxygen flux; (N = 6/group). (F) Metabolomics analysis demonstrating enrichment for glycolysis (red dots), ketone (green dot), glycogen (maroon dot), TCA cycle (orang dot) and AMP (black dot) metabolites in ACHD hearts at 8 weeks (N = 6). (G) Up-regulated metabolites and processes shown in F highlighted in green. (H) Western blot and quantification of enzymes associated with glucose (PDH), FOA (CPT-1), ketone (BDH1) and energy sensing (AMPK/phospho-AMPK) (N = 3). Results shown as Mean ± SEM, Student's t-test, *p < 0.05, ****p < 0.0001.

increase in glycolysis and a small decrease in ketone and fatty acid oxidation (FAO) metabolites in ACHD hearts (Figure 4F,G and Supplementary Table 3), in particular glucose-1P, glucose 6-P, fructose 6-P for glycolysis and 3-hydroxybutyric acid for ketone metabolism. Furthermore, AMP levels were increased in ACHD hearts but this alteration did not trigger differential AMPK activation (Figure 4G,H), suggestive of failure to respond to energetic imbalance in mutant hearts. Metabolomic changes were further confirmed by western blot of heart samples, which revealed a significant increase in PDH (Glucose metabolism), small decrease in CPT1 (Fatty Acid metabolism) and BDH (Ketone metabolism) (Figure 4H). These data suggest a shift from FAO towards increased glycolysis in ACHD myocytes, reminiscent of the fetal energetic program. Increased glucose dependency is an adaptive response to maintain heart function under stress conditions [32,39,40]. The observed changes in cardiomyocyte energetic pathways indicate that disturbances in metabolic state precede heart dysfunction in ACHD and therefore represent valuable parameters to measure predisposition to heart failure.

3.6. Intervention on energy metabolism by metformin prevents cardiac dysfunction in ACHD

Given the newly identified role for *Nkx2-5* in regulating metabolism in ACHD hearts, we tested if early pharmacological intervention on global metabolism could prevent heart disease progression in ACHD mice. Young mice under HF diet were treated with metformin, a widely used FDA-approved drug used to treat type 2 diabetes (Figure 5A). Metformin acts by improving metabolism and increasing glucose sensitivity, FAO utilization, and mitochondrial function [41], all processes

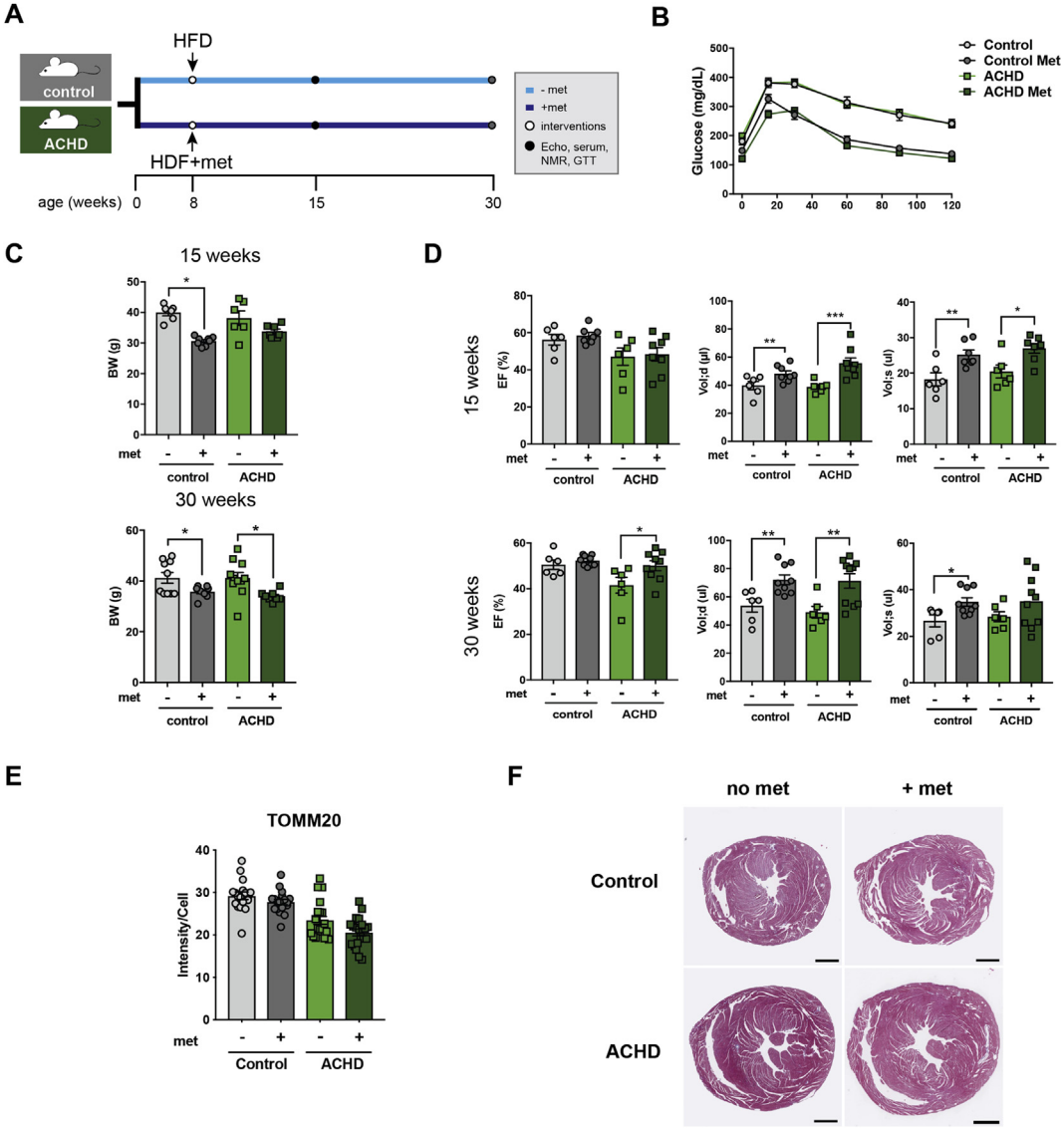

Figure 5: Heart function and body metabolism in metformin treated animals under HF diet. (A) Experimental design and HF diet/metformin treatment groups. (B) Glucose handling in ACHD and control mice under metformin treatment at 30 weeks. (C) Body weight measurements of control and ACHD mice under metformin treatment at the early (15-week) and long (30-week) treatment regimens. (D) Cardiac function in control and ACHD mice treated with metformin at 15 and 30 weeks under HF diet (N = 6). (E) Quantification of mitochondrial density using immunofluorescence for TOMM20 (N = 2) in control and ACHD animals under metformin treatment (N = 2). (F) Trichrome staining of transverse heart sections. Data shown as Mean ± SEM, Student's t-test, *p < 0.05, **p < 0.01; ***p < 0.001. HFD – high fat diet; Met – metformin; BW – body weight; EF – left ventricular ejection fraction; Vol;d – left ventricular end diastolic volume; Vol;s – left ventricular end systolic volume.

found dysregulated in ACHD hearts. Both control and ACHD mice treated with metformin showed significant decrease in basal levels of glucose during fasting and improvement in glucose handling (Figure 5B). Normalization of glucose tolerance curves by basal glucose levels showed that ACHD mice initially display better glucose handling when compared to control mice, but metformin treatment had no effect on ACHD mice (Supplementary Figure 8). During metformin treatment, an early effect in fat mass gain (not shown) was seen in control mice only (15 weeks of age; 9 weeks of treatment), while both control and ACHD mice showed reduced body weight with longer treatment (30 weeks of age; 22 weeks of treatment) (Figure 5C). Early differences in weight loss between control and ACHD animals might reflect differential glucose metabolism (Figure 2B). As detected earlier, ACHD mice at 15 weeks had a small decrease in EF when compared to control. Short metformin treatment led to increased diastolic and systolic volumes that were independent of genotype (Figure 5D, upper panel). At 30 weeks of age (22 weeks of treatment) metformin treatment reverted heart dysfunction on ACHD mice, normalizing EF to control levels by changes in both diastolic and systolic functions when compared to no-metformin ACHD mice (Figure 5D, lower panel). ACHD hearts maintained structural (hypertrophy, Figure 5E) and metabolic (mitochondrial content, Figure 5F) abnormalities upon long-term metformin treatment. Serum analysis of lipids showed that metformin treated mice displayed decrease in circulating cholesterol (CHOL) and free fatty acids (NEFA), while no significant changes were seen in triglycerides (Figure 6A, upper panel). Again, no significant differences were seen between control and ACHD mice. As previously seen, ACHD mice display lower glucose basal levels when compared to control. Under metformin treatment, a significant decrease in glucose was seen in controls, while decreases in ACHD mice did not reached significance (Figure 6A, lower left panel). It is important to note that not all animals reacted to metformin treatment; 2/6 in control; $^{1}/_{4}$ in ACHD were outliers and still showed high levels of circulating glucose. Chronic exposure to high fat diet has been associated with increased lipid liver deposition, leading to non-alcoholic fatty liver disease (NAFLD) that can progress to hepatic steatosis. Chronic treatment with metformin was able to revert fat deposition in both control and ACHD mice, leading to decreased LDH and SDH serum levels (Figure 6A, left panels), decreased steatosis (Figure 6B) and increased glycogen accumulation in the liver (Figure 6C). These data demonstrate that modulation of energy metabolism by metformin, acting both at the liver and heart, can be safely used for treatment of cardiac dysfunction mediated by obesity in ACHD.

4. DISCUSSION

Using murine modeling, we demonstrate that changes in energy flexibility is a hallmark of ACHD hearts at early adulthood, and that

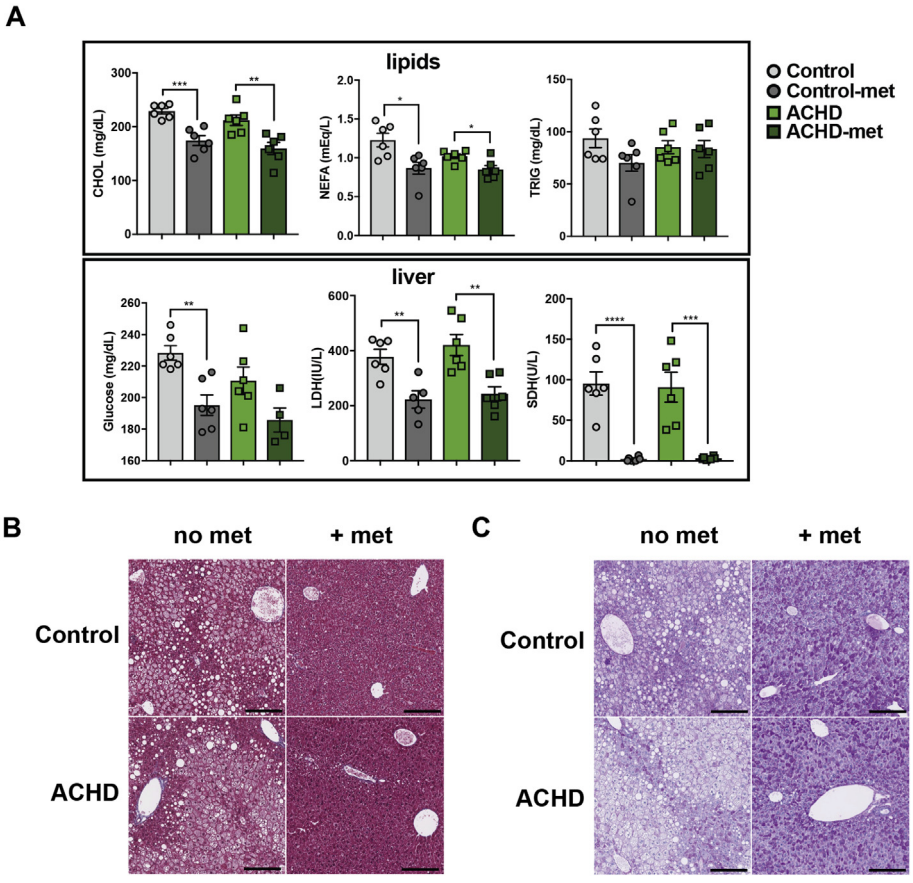

Figure 6: Liver damage in metformin treated animals under HF diet. (A) Serum analysis of 30 week high fat-diet control and ACHD mice showing levels of circulating lipids, i.e. cholesterol (CHOL), non-esterified fatty acids (NEFA) and triglycerides (TRIG), as well as measurements of liver function glucose, lactate dehydrogenase (LDH) and sorbitol dehydrogenase (SHD). (B) Histological liver sections showing pathology of control and ACHD animals under HF diet with or without metformin treatment. Pale areas denote macro and micro lipid vesicles. (C) Periodic Acid Schiff (PAS) staining of control and ACHD liver sections shows staining for glycogen (dark purple). Data shown as Mean ± SEM, Student's t-test, *p < 0.05, **p < 0.01; ***p < 0.001, ****p < 0.0001. Met – metformin.

metabolic imbalance is strongly associated with the progression to heart ACHD heart dysfunction in obesity. Our data show a series of alterations in metabolic substrates that precede cardiac dysfunction in ACHD mice and that pharmacological intervention with metformin can be used to prevent pathological metabolic changes and consequently retain normal heart function. By demonstrating that *Nkx2-5* mutations, known to cause congenital cardiac malformations, are responsible for primary defects in the metabolic capacity of the heart, this study highlights how CHD genes can directly impact cardiac energy utilization. The heart is very sensitive to metabolic imbalance; given the low oxygen and high glucose availability provided by the mother, embryonic and early neonatal hearts display a high dependence on glycolysis. After birth, cardiac metabolism is shifted to fatty acid, which is a more efficient source of energy to sustain the increased mechanical demand of the adult heart [42]. Although >95% of the ATP produced in the adult heart derives from oxidative phosphorylation, energetic flexibility is essential for adaptation of heart function to physiological changes. Decreased flexibility is also associated with pathological states [39,42], as energy products such as ATP, acetyl-CoA and diacylglycerides directly impact on heart contractility and act as second messengers controlling heart function [39].

Given the high energetic demand of the heart and the mitochondrial role in controlling energy consumption, generation of reactive oxygen species and apoptosis, mitochondrial defects are strongly associated with cardiac dysfunction [43]. The decreased mitochondrial density in ACHD hearts suggests a primary defect in mitochondrial biogenesis, in which further investigation is merited. Mitochondrial dysfunction is also supported by the observed decrease in cellular respiration and impaired energetics in ACHD hearts, where early changes in cardiac metabolism lead to increased dependency on glycolysis and decreased metabolic flexibility. Altered glucose metabolism is one of the drivers of the hypertrophic response and an early marker of heart disease progression [44], which could be adaptive under a homeostatic condition, but triggers heart dysfunction once a second metabolic stress (such as obesity) is imposed.

Despite the extensive energetic abnormalities in ACHD hearts, no evidence of lipotoxicity was found in histological analyses of heart sections (not shown), although important changes in lipid distribution were detected in the metabolomic analyses. Given the decreased energetic flexibility and fatty acid oxidation coupled with increased fatty acid availability in ACHD/obesity, it is possible that lipotoxicity may play a role in the later stages of disease progression.

In addition to intrinsic cardiac structural and metabolic changes, there is a strong possibility that other extrinsic changes to the heart may contribute to the cardiac dysfunction in our ACHD/obesity model. The full knockin approach used in this work mimics the pathology of the mutation in the heart but also affects other sites where *Nkx2-5* is expressed, including the tongue, thyroid, central nervous system, thymus liver, spleen and gut, among others, when enzymatic techniques are used for amplification of signal detection, such as in situ hybridization and transgenic beta-galactosidase while in adults cardiac expression is highly predominant [45–47]. Such sites are normally neglected when cardiovascular analyses are performed. In the thyroid, *Nkx2-5* is transiently expressed during early development and has shown to control thyroid gene expression [48,49]. *Nkx2-5* mutations outside of the homeodomain have been linked to thyroid dysmorphogenesis in patients [49]. We are currently investigating the role of *Nkx2-5* in thyroid development and heart function using conditional deletion approaches. Preliminary analysis of hematocrit in ACHD adult mice has shown no significant differences in blood cell composition (data not shown). It is also possible *de novo* expression of *Nkx2-5* in disease states modifies the cardiovascular phenotype, as seen in atherosclerotic plaques in ApoE–deficient mice and patients with pulmonary hypertension [50,51]. However, mice do not normally develop atherosclerosis. Despite these caveats, our work strongly supports a direct action of *Nkx2-5* as a controller of heart metabolism. Metformin has known cardioprotective effects and limits cardiovascular events in patients [52,53], regulating global and tissue metabolism via complex mechanisms that are not completely understood. Metformin also acts by reducing hepatic glucose production by the gut and by increasing glucose organ sensitivity [54], and has been previously shown to protect against cancer in NAFLD models [55–57]. Despite our best efforts, we have not detected any global metabolic or structural cardiac changes associated with the improved ACHD heart function upon metformin treatment in our model. Furthermore, the known action of metformin in the liver, also detected in this study, might contribute to the cardioprotective action on the treatment. Other possible mechanisms of action are currently under investigation in our group. At the cellular level, metformin likely acts via AMPK-dependent and -independent mechanisms to modulate mitochondrial and lysosome function [41]. Interestingly, despite the early detection of high levels of ATP in ACHD hearts at 8 weeks, no changes in AMPK were detected, suggesting a possible impairment of the AMPK signaling pathway, or an AMPK-independent mechanism of action (Figure 4G,H). Recent studies have shown that chronic exposure to metformin increases lifespan in mice [58,59] and has beneficial effects in cancer treatments [60] and cardiovascular dysfunction [52,61–64], albeit some divergence between preclinical and clinical trials for metformin in humans have been described as seen for non-diabetic STEMI patients [53]. Cellular uptake of metformin is controlled by organic cation transporters (OCT) belonging to the *Slc22a* gene family. Expression of OCT1 and OCT3 have been described in the heart [65]. Future studies are necessary to establish the tissue-specific action of global metformin administration to mice and cardiac-intrinsic mechanisms determining beneficial effects of metformin treatment in ACHD.

5. CONCLUSIONS

The increased prevalence of ACHD in the population [1,2,66] and its association with metabolic syndrome [67] call for mechanistic studies to understand how cardiac energy flexibility correlates with heart function in homeostasis and disease [39,68,69]. Surveillance of cardiac performance combined with modulation of energy utilization could lead to improvement of heart function and prevent heart failure in ACHD, as demonstrated in this study using murine modeling. More effective treatments for heart failure should move focus from solely examining neurohormonal/unloading modulation to including corrections for metabolically affected hearts [70]. The findings presented here argue for manipulation of energy metabolism and mitochondrial function as potential intervention targets to revert progression to heart failure in ACHD.

ACKNOWLEDGMENTS

We thank Pete A. Williams for providing mitochondrial antibodies and advice, and the *In Vivo* Physiology, histology and microscopy cores of the Jackson Laboratory for the generation of all metabolic and physiological data.

SOURCE OF FUNDING

The Australian Regenerative Medicine Institute is supported by grants from the State Government of Victoria and the Australian Government. JCW was supported by

Konrad-Adenauer-Stiftung e.V. JTP was supported by an intramural grant of National Cerebral & Cardiovascular Center (27-2-2). This work was funded by NHMRC Project grant 1069710 to MWC, MR and NAR; NHMRC-Australia Fellowship to NAR, NHMRC/NHF 1049980 CDF to MR, and ARC Stem Cells Australia to NAR and Saving Tiny Hearts Society grant to MWC.

AUTHOR CONTRIBUTIONS

Conceptualization, MWC and MBF; Methodology, JCW, MBF, and MWC; Formal Analysis, GC, PB, VP, DC, HK, SA, and MR; Investigation, JCW, RP, AC, OH, EF, JS, QW, JTP, MBF, and MWC; Writing — original draft, JCW, MBF, and MWC; Writing — Review and Editing, JH, HHP, NAR MBF, and MWC; Funding Acquisition, NAR. and MWC; Supervision, MBF, JH, NAR, and MWC.

CONFLICT OF INTEREST

The authors declare that they have no conflict of interests.

APPENDIX A. SUPPLEMENTARY DATA

Supplementary data to this article can be found online at https://doi.org/10.1016/j.molmet.2018.11.002.

REFERENCES

[1] Alshawabkeh, L.I., Opotowsky, A.R., 2016. Burden of heart failure in adults with congenital heart disease. Current Heart Failure Reports 13(5):247—254.
[2] Marelli, A.J., Ionescu-Ittu, R., Mackie, A.S., Guo, L., Dendukuri, N., Kaouache, M., 2014. Lifetime prevalence of congenital heart disease in the general population from 2000 to 2010. Circulation 130(9):749—756.
[3] Lui, G.K., Saidi, A., Bhatt, A.B., Burchill, L.J., Deen, J.F., Earing, M.G., et al., 2017. Diagnosis and management of noncardiac complications in adults with congenital heart disease: a scientific statement from the American Heart Association. Circulation 136(20):e348—e392.
[4] Ogden, C.L., Carroll, M.D., Kit, B.K., Flegal, K.M., 2014. Prevalence of childhood and adult obesity in the United States, 2011—2012. Journal of the American Medical Association 311(8):806—814.
[5] Writing Group, M., Mozaffarian, D., Benjamin, E.J., Go, A.S., Arnett, D.K., Blaha, M.J., et al., 2016. Executive summary: heart disease and stroke statistics–2016 update: a report from the American Heart Association. Circulation 133(4):447—454.
[6] Roche, S.L., Silversides, C.K., 2013. Hypertension, obesity, and coronary artery disease in the survivors of congenital heart disease. Canadian Journal of Cardiology 29(7):841—848.
[7] Islam, S., Yasui, Y., Kaul, P., Mackie, A.S., 2016. Hospital readmission of patients with congenital heart disease in Canada. Canadian Journal of Cardiology 32(8), 987 e7—987 e14.
[8] Costa, M.W., Guo, G., Wolstein, O., Vale, M., Castro, M.L., Wang, L., et al., 2013. Functional characterization of a novel mutation in NKX2-5 associated with congenital heart disease and adult-onset cardiomyopathy. Circulation: Cardiovascular Genetics 6(3):238—247.
[9] Furtado, M.B., Wilmanns, J.C., Chandran, A., Perera, J., Hon, O., Biben, C., et al., 2017. Point mutations in murine Nkx2-5 phenocopy human congenital heart disease and induce pathogenic Wnt signaling. JCI Insight 2(6):e88271.
[10] Heiberg, E., Sjogren, J., Ugander, M., Carlsson, M., Engblom, H., Arheden, H., 2010. Design and validation of segment — freely available software for cardiovascular image analysis. BMC Medical Imaging 10:1.
[11] Gnaiger, E., Kuznetsov, A.V., Schneeberger, S., Seiler, R., Brandacher, G., Steurer, W., et al., 2000. Mitochondria in the cold. In: Heldmaier, G., Klingenspor, M. (Eds.), Life in the cold. Heidelberg, Berlin, New York: Springer. p. 431—42.
[12] Schopf, B., Schafer, G., Weber, A., Talasz, H., Eder, I.E., Klocker, H., et al., 2016. Oxidative phosphorylation and mitochondrial function differ between human prostate tissue and cultured cells. FEBS Journal 283(11):2181—2196.
[13] Xia, J., Wishart, D.S., 2016. Using MetaboAnalyst 3.0 for comprehensive metabolomics data analysis. Current Protocols in Bioinformatics 55:14.10.1—14.10.91.
[14] Hackstadt, A.J., Hess, A.M., 2009. Filtering for increased power for microarray data analysis. BMC Bioinformatics 10:11.
[15] Dieterle, F., Ross, A., Schlotterbeck, G., Senn, H., 2006. Probabilistic quotient normalization as robust method to account for dilution of complex biological mixtures. Application in 1H NMR metabonomics. Analytical Chemistry 78(13):4281—4290.
[16] van den Boogaard, M., Wong, L.Y., Tessadori, F., Bakker, M.L., Dreizehnter, L.K., Wakker, V., et al., 2012. Genetic variation in T-box binding element functionally affects SCN5A/SCN10A enhancer. Journal of Clinical Investigation 122(7):2519—2530.
[17] McLean, C.Y., Bristor, D., Hiller, M., Clarke, S.L., Schaar, B.T., Lowe, C.B., et al., 2010. GREAT improves functional interpretation of cis-regulatory regions. Nature Biotechnology 28(5):495—501.
[18] Martin, M., 2011. Cutadapt removes adapter sequences from high-throughput sequencing reads. EMBnet.journal 17(1):10—12.
[19] Dobin, A., Davis, C.A., Schlesinger, F., Drenkow, J., Zaleski, C., Jha, S., et al., 2013. STAR: ultrafast universal RNA-seq aligner. Bioinformatics 29(1):15—21.
[20] Anders, S., Pyl, P.T., Huber, W., 2015. HTSeq — a Python framework to work with high-throughput sequencing data. Bioinformatics 31(2):166—169.
[21] Law, C.W., Chen, Y., Shi, W., Smyth, G.K., 2014. voom: precision weights unlock linear model analysis tools for RNA-seq read counts. Genome Biology 15(2):R29.
[22] Ferrari, R., Bohm, M., Cleland, J.G., Paulus, W.J., Pieske, B., Rapezzi, C., et al., 2015. Heart failure with preserved ejection fraction: uncertainties and dilemmas. European Journal of Heart Failure 17(7):665—671.
[23] Graham, L.C., Harder, J.M., Soto, I., de Vries, W.N., John, S.W., Howell, G.R., 2016. Chronic consumption of a western diet induces robust glial activation in aging mice and in a mouse model of Alzheimer's disease. Scientific Reports 6:21568.
[24] Dai, Y.S., Cserjesi, P., Markham, B.E., Molkentin, J.D., 2002. The transcription factors GATA4 and dHAND physically interact to synergistically activate cardiac gene expression through a p300-dependent mechanism. Journal of Biological Chemistry 277(27):24390—24398.
[25] Dirkx, E., Gladka, M.M., Philippen, L.E., Armand, A.S., Kinet, V., Leptidis, S., et al., 2013. Nfat and miR-25 cooperate to reactivate the transcription factor Hand2 in heart failure. Nature Cell Biology 15(11):1282—1293.
[26] Hartmann, S., Ridley, A.J., Lutz, S., 2015. The function of Rho-associated kinases ROCK1 and ROCK2 in the pathogenesis of cardiovascular disease. Frontiers in Pharmacology 6:276.
[27] Heineke, J., Molkentin, J.D., 2006. Regulation of cardiac hypertrophy by intracellular signalling pathways. Nature Reviews Molecular Cell Biology 7(8):589—600.
[28] Yanazume, T., Hasegawa, K., Morimoto, T., Kawamura, T., Wada, H., Matsumori, A., et al., 2003. Cardiac p300 is involved in myocyte growth with decompensated heart failure. Molecular and Cellular Biology 23(10):3593—3606.
[29] Djouadi, F., Weinheimer, C.J., Saffitz, J.E., Pitchford, C., Bastin, J., Gonzalez, F.J., et al., 1998. A gender-related defect in lipid metabolism and glucose homeostasis in peroxisome proliferator- activated receptor alpha-deficient mice. Journal of Clinical Investigation 102(6):1083—1091.
[30] Luptak, I., Balschi, J.A., Xing, Y., Leone, T.C., Kelly, D.P., Tian, R., 2005. Decreased contractile and metabolic reserve in peroxisome proliferator-

activated receptor-alpha-null hearts can be rescued by increasing glucose transport and utilization. Circulation 112(15):2339–2346.

[31] Lopaschuk, G.D., Ussher, J.R., Folmes, C.D., Jaswal, J.S., Stanley, W.C., 2010. Myocardial fatty acid metabolism in health and disease. Physiological Reviews 90(1):207–258.

[32] Aubert, G., Martin, O.J., Horton, J.L., Lai, L., Vega, R.B., Leone, T.C., et al., 2016. The failing heart relies on ketone bodies as a fuel. Circulation 133(8): 698–705.

[33] Ventura-Clapier, R., Garnier, A., Veksler, V., 2004. Energy metabolism in heart failure. The Journal of Physiology 555(Pt 1):1–13.

[34] Doenst, T., Nguyen, T.D., Abel, E.D., 2013. Cardiac metabolism in heart failure: implications beyond ATP production. Circulation Research 113(6): 709–724.

[35] Chowdhury, R., Ashraf, H., Melanson, M., Tanada, Y., Nguyen, M., Silberbach, G.M., et al., 2015. A mouse model of human congenital heart disease: progressive atrioventricular block induced by a heterozygous Nkx2-5 homeodomain missense mutation. Circulation Arrhythmia and Electrophysiology 8(5):1255–1264.

[36] Gutierrez-Roelens, I., Sluysmans, T., Gewillig, M., Devriendt, K., Vikkula, M., 2002. Progressive AV-block and anomalous venous return among cardiac anomalies associated with two novel missense mutations in the CSX/NKX2-5 gene. Human Mutation 20(1):75–76.

[37] Jay, P.Y., Harris, B.S., Maguire, C.T., Buerger, A., Wakimoto, H., Tanaka, M., et al., 2004. Nkx2-5 mutation causes anatomic hypoplasia of the cardiac conduction system. Journal of Clinical Investigation 113(8):1130–1137.

[38] Pashmforoush, M., Lu, J.T., Chen, H., Amand, T.S., Kondo, R., Pradervand, S., et al., 2004. Nkx2-5 pathways and congenital heart disease; loss of ventricular myocyte lineage specification leads to progressive cardiomyopathy and complete heart block. Cell 117(3):373–386.

[39] Ritterhoff, J., Tian, R., 2017. Metabolism in cardiomyopathy: every substrate matters. Cardiovascular Research 113(4):411–421.

[40] Taegtmeyer, H., Young, M.E., Lopaschuk, G.D., Abel, E.D., Brunengraber, H., Darley-Usmar, V., et al., 2016. Assessing cardiac metabolism: a scientific statement from the American Heart Association. Circulation Research 118(10): 1659–1701.

[41] Rena, G., Hardie, D.G., Pearson, E.R., 2017. The mechanisms of action of metformin. Diabetologia 60(9):1577–1585.

[42] Wende, A.R., Brahma, M.K., McGinnis, G.R., Young, M.E., 2017. Metabolic origins of heart failure. JACC: Basic to Translational Science 2(3):297–310.

[43] Huss, J.M., Kelly, D.P., 2005. Mitochondrial energy metabolism in heart failure: a question of balance. Journal of Clinical Investigation 115(3):547–555.

[44] Kundu, B.K., Zhong, M., Sen, S., Davogustto, G., Keller, S.R., Taegtmeyer, H., 2015. Remodeling of glucose metabolism precedes pressure overload-induced left ventricular hypertrophy: review of a hypothesis. Cardiology 130(4):211–220.

[45] Diez-Roux, G., Banfi, S., Sultan, M., Geffers, L., Anand, S., Rozado, D., et al., 2011. A high-resolution anatomical atlas of the transcriptome in the mouse embryo. PLoS Biology 9(1):e1000582.

[46] Komuro, I., Izumo, S., 1993. Csx: a murine homeobox-containing gene specifically expressed in the developing heart. Proceedings of the National Academy of Sciences of the United States of America 90(17):8145–8149.

[47] Stanley, E.G., Biben, C., Elefanty, A., Barnett, L., Koentgen, F., Robb, L., et al., 2002. Efficient Cre-mediated deletion in cardiac progenitor cells conferred by a 3'UTR-ires-Cre allele of the homeobox gene Nkx2-5. International Journal of Developmental Biology 46(4):431–439.

[48] Cardoso-Weide, L.C., Cardoso-Penha, R.C., Costa, M.W., Ferreira, A.C., Carvalho, D.P., Santisteban, P.S., 2015. DuOx2 promoter regulation by hormones, transcriptional factors and the coactivator TAZ. European Thyroid Journal 4(1):6–13.

[49] Dentice, M., Cordeddu, V., Rosica, A., Ferrara, A.M., Santarpia, L., Salvatore, D., et al., 2006. Missense mutation in the transcription factor NKX2-5: a novel molecular event in the pathogenesis of thyroid dysgenesis. The Journal of Clinical Endocrinology and Metabolism 91(4):1428–1433.

[50] Dritsoula, A., Papaioannou, I., Guerra, S.G., Fonseca, C., Martin, J., Herrick, A.L., et al., 2018. Molecular basis for dysregulated activation of NKX2-5 in the vascular remodeling of systemic sclerosis. Arthritis & Rheumatology 70(6):920–931.

[51] Du, M., Wang, X., Tan, X., Li, X., Huang, D., Huang, K., et al., 2016. Nkx2-5 is expressed in atherosclerotic plaques and attenuates development of atherosclerosis in apolipoprotein E-deficient mice. Journal of the American Heart Association 5(12).

[52] Eppinga, R.N., Kofink, D., Dullaart, R.P., Dalmeijer, G.W., Lipsic, E., van Veldhuisen, D.J., et al., 2017. Effect of metformin on metabolites and relation with myocardial infarct size and left ventricular ejection fraction after myocardial infarction. Circulation. Cardiovascular Genetics 10(1).

[53] Lexis, C.P., van der Horst, I.C., Lipsic, E., Wieringa, W.G., de Boer, R.A., van den Heuvel, A.F., et al., 2014. Effect of metformin on left ventricular function after acute myocardial infarction in patients without diabetes: the GIPS-III randomized clinical trial. Journal of the American Medical Association 311(15):1526–1535.

[54] Pernicova, I., Korbonits, M., 2014. Metformin — mode of action and clinical implications for diabetes and cancer. Nature Reviews Endocrinology 10(3): 143–156.

[55] Kim, E.K., Lee, S.H., Jhun, J.Y., Byun, J.K., Jeong, J.H., Lee, S.Y., et al., 2016. Metformin prevents fatty liver and improves balance of white/brown adipose in an obesity mouse model by inducing FGF21. Mediators of Inflammation 2016: 5813030.

[56] Riera-Borrull, M., Garcia-Heredia, A., Fernandez-Arroyo, S., Hernandez-Aguilera, A., Cabre, N., Cuyas, E., et al., 2017. Metformin potentiates the benefits of dietary restraint: a metabolomic study. International Journal of Molecular Sciences 18(11).

[57] Tajima, K., Nakamura, A., Shirakawa, J., Togashi, Y., Orime, K., Sato, K., et al., 2013. Metformin prevents liver tumorigenesis induced by high-fat diet in C57Bl/6 mice. American Journal of Physiology. Endocrinology and Metabolism 305(8):E987–E998.

[58] Martin-Montalvo, A., Mercken, E.M., Mitchell, S.J., Palacios, H.H., Mote, P.L., Scheibye-Knudsen, M., et al., 2013. Metformin improves healthspan and lifespan in mice. Nature Communications 4:2192.

[59] Valencia, W.M., Palacio, A., Tamariz, L., Florez, H., 2017. Metformin and ageing: improving ageing outcomes beyond glycaemic control. Diabetologia 60(9):1630–1638.

[60] Heckman-Stoddard, B.M., DeCensi, A., Sahasrabuddhe, V.V., Ford, L.G., 2017. Repurposing metformin for the prevention of cancer and cancer recurrence. Diabetologia 60(9):1639–1647.

[61] Griffin, S.J., Leaver, J.K., Irving, G.J., 2017. Impact of metformin on cardiovascular disease: a meta-analysis of randomised trials among people with type 2 diabetes. Diabetologia 60(9):1620–1629.

[62] Kobashigawa, L.C., Xu, Y.C., Padbury, J.F., Tseng, Y.T., Yano, N., 2014. Metformin protects cardiomyocyte from doxorubicin induced cytotoxicity through an AMP-activated protein kinase dependent signaling pathway: an in vitro study. PLoS One 9(8):e104888.

[63] Sun, D., Yang, F., 2017. Metformin improves cardiac function in mice with heart failure after myocardial infarction by regulating mitochondrial energy metabolism. Biochemical and Biophysical Research Communications 486(2):329–335.

[64] Tzanavari, T., Varela, A., Theocharis, S., Ninou, E., Kapelouzou, A., Cokkinos, D.V., et al., 2016. Metformin protects against infection-induced myocardial dysfunction. Metabolism 65(10):1447–1458.

[65] Lozano, E., Briz, O., Macias, R.I.R., Serrano, M.A., Marin, J.J.G., Herraez, E., 2018. Genetic heterogeneity of SLC22 family of transporters in drug disposition. Journal of Personalized Medicine 8(2).

[66] Gilboa, S.M., Devine, O.J., Kucik, J.E., Oster, M.E., Riehle-Colarusso, T., Nembhard, W.N., et al., 2016. Congenital heart defects in the United States:

estimating the magnitude of the affected population in 2010. Circulation 134(2):101–109.

[67] Deen, J.F., Krieger, E.V., Slee, A.E., Arslan, A., Arterburn, D., Stout, K.K., et al., 2016. Metabolic syndrome in adults with congenital heart disease. Journal of the American Heart Association 5(2):e001132.

[68] Goodpaster, B.H., Sparks, L.M., 2017. Metabolic flexibility in health and disease. Cell Metabolism 25(5):1027–1036.

[69] Neglia, D., De Caterina, A., Marraccini, P., Natali, A., Ciardetti, M., Vecoli, C., et al., 2007. Impaired myocardial metabolic reserve and substrate selection flexibility during stress in patients with idiopathic dilated cardiomyopathy. American Journal of Physiology: Heart and Circulatory Physiology 293(6):H3270–H3278.

[70] Brown, D.A., Perry, J.B., Allen, M.E., Sabbah, H.N., Stauffer, B.L., Shaikh, S.R., et al., 2017. Expert consensus document: mitochondrial function as a therapeutic target in heart failure. Nature Reviews Cardiology 14(4):238–250.

